Romanian Reports in Physics, Vol. 59, No. 2, P. 433–446, 2007

Dedicated to Prof. Dorin N. Poenaru's 70th Anniversary, my father and my mentor

MICROSCOPIC NECKING POTENTIAL FOR BINARY PROCESSES

R.A. GHERGHESCU[1,2]

[1] *Frankfurt Institute for Advanced Studies, J.W. Goethe University*
Max-von-Laue-Str. 1, D-60438 Frankfurt am Main, Germany
E-mail: author1@fias.uni-frankfurt.de
[2] *National Institute for Nuclear Physics and Engineering*
P.O. Box MG-6, RO-077125 Bucharest-Magurele, Romania
E-mail: radu@radu.nipne.ro

(Received February 15, 2007)

Abstract. A specialized potential is derrived from the potential theory using an oscillator type force as being reponsable for the confining of the nucleons into the necking region. The necking potential perfectly reproduces the concave smoothing surface which ensures shape continuity from one spheroidal fragment to the other. It also introduces a new degree of freedom as the radius of the neck generating sphere. Single particle levels are obtain for different neck radii and their influence on the proton and neutron shell corrections is calculated.

Key words: single-particle levels, shell corrections.

1. INTRODUCTION

This work is fulfilling an adequate description of microscopic potential which appears in binary processes such as cold fission, cluster radioactivities and alpha decay in terms of an asymmetric and deformed single particle shell model with more realistic shapes.

Many attempts have been made to use the two-center shell model in synthesis and decay of nuclei. This model is theoretically suitable for the study of microscopic effects on daughter-emitted fragment configuration in their way from one single quantum system to two completely separated. The transition behaviour of the two partner shells, both protonic and neutronic,

is able to lower the potential barrier of the process by taking into account the neck degree of freedom as a free parameter. In any process which implies a pass from one quantum system to two, such as fission, there are certain situations when one or both fission fragments are deformed. The importance of an adequate description of cold fission, cluster radioactivities and alpha decay in terms of an asymmetric and *deformed* single particle shell model with more realistic shapes during fission and fusion processes was repeteadly stressed [1]. Such a reaction could yield cold energy valleys due to deformed shell structure of the participants [2]. Fragments deformation is properly taken into account in this work. A very complete two-center shell model (DTCSM) is proposed, where the main part of the potential consists of two spheroidally deformed Nilsson type oscillators for axially symmetric shapes. Any change in the nuclear surface shape is reflected in a corresponding modification of the four oscillator frequencies along the symmetry axis and perpendicular to it.

It is also established that, especially in fission and cluster decay, a necking region builds its way between the fragments, smoothly linking the two spheroids one to the other. This work associates for the first time a microscopic potential to a spherically matching neck region of the nuclear shape. The neck potential is constructed in such a way that it takes the same value on the necking region surface as on the spheroidal surfaces of the fragments. Equipotentiality is thus respected on the nuclear surface.

The usual spin-orbit and squared angular momentum operators are calculated with help of the potential-dependent formulae $\mathbf{ls} = (\nabla V \times \mathbf{p})\mathbf{s}$, and $\mathbf{l}^2 = (\nabla V \times \mathbf{p})^2$ [4]. The potential in this model follows exactly the nuclear shape, and so do the $\mathbf{ls}$ and $\mathbf{l}^2$ operators. Finally, the levels diagram with respect to the elongation, neck parameter and fragment deformations are used to calculate the shell correction by means of the Strutinsky method. The smoothing procedure is used as prescribed in [3].

2. BINARY SHAPES

The model presented in this work is treating axially symmetric shapes. Two spheroids (the deformed fragments) with semiaxes a_1, b_1 and a_2, b_2 are, at a certain moment, separated at a distance R between the two centers O_1 and O_2. A sphere centered in O_3 with radius R_3 is rolling around the symmetry axis, being tangent all the time to the two ellipsoids. The necking region, between the two tangent points, is generated in this way. Thus we have five independent parameters to design the deformation space: two fragment shape asymmetries $\chi_1 = b_1/a_1$, $\chi_2 = b_2/a_2$ (if a_1 and a_2 are given as the correspondent of β_2 for every A_1 and A_2, the other semiaxes are calculated from

the total volume conservation condition), mass asymmetry A_1/A_2, the neck radius R_3 and the distance between centers R. Obviously, this set is available for every parent nucleus A, Z with its own $\chi = b/a$. A few shape sequences obtained by varying two of the parameters, R_3 and R for the same parent and the same mass asymmetry A_1/A_2 are depicted in Fig. 1. Every row starts with the same spheroidal parent on the left hand side of the figure. As the distance between centers increases, the two deformed fragments with fixed χ_1 and χ_2 shape asymmetries begin to separate one from the other. Variation with the neck radius R_3 is noticeable on vertical direction. Shape sequences with very small necking region are shown in the upper row (for zero neck radius, $R_3 = 0$ fm, we get compact shapes suitable for fusion reactions), passing through intermediary neck radii, comparable to the magnitude of the ellipsoids semiaxes (second and third row), down to the last row where large neck radius generates very elongated shapes.

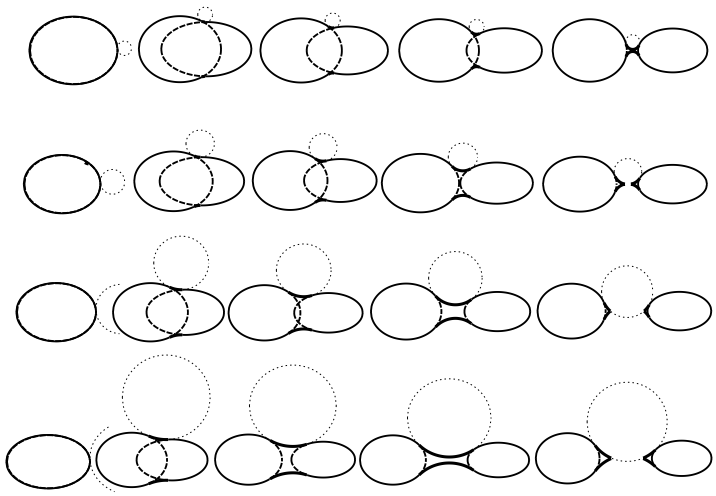

Fig. 1 – Sequence of shapes for different neck radius values within the shape evolution along distance between centers.

This kind of configurations will be microscopically treated along the variation of the deformation space parameters.

3. THE MICROSCOPIC POTENTIAL

A microscopic potential accounting for the perfect description of the binary nuclear configuration shell be derrived in this section.

The equations for shape surfaces described in the previous section can be written in cylindrical coordinates (due to axyal symmetry) as:

$$\rho(z) = \begin{cases} \rho_1(z) = [b_1^2 - \chi_1^2 z^2]^{1/2}, & -a_1 \le z \le z_{c1} \\ \rho_g(z) = \rho_3 - [R_3^2 - (z - z_3)^2]^{1/2}, & z_{c1} \le z \le z_{c2} \\ \rho_2(z) = [b_2^2 - \chi_2^2 (z - R)^2]^{1/2}, & z_{c2} \le z \le R + a_2, \end{cases} \tag{1}$$

where the origin is placed in the center of the heavy fragment O_1. Neck sphere center coordinates are (z_3, ρ_3), and z_{c1} and z_{c2} are the two tangent points of the neck sphere with the two spheroids.

The oscillator potential correspondig to these two-center shapes must have the same value on the nuclear surface. For spheres, for example we have:

$$V_0 = \frac{m_0 \omega_i^2 R_i^2}{2}, \tag{2}$$

where R_i is the radii of a nucleus with atomic mass A_i. Since $\hbar\omega_i = 41 A^{-1/3}$ and $R_i = r_0 A^{1/3}$ (where $r_0 \approx 1.16$), then $V_0 \approx 54.5$ MeV. If we write these simple relations for the surface of ellipsoidal shapes:

$$\frac{1}{2} m_0 \omega_{z_i}^2 a_i^2 = V_0, \quad \frac{1}{2} m_0 \omega_{\rho_i}^2 b_i^2 = V_0, \tag{3}$$

the frequencies ω_{z_i}, ω_{ρ_i} are defined along the symmetry axis and respectively perpendicular to it, as functions of the two ellipse semiaxes.

For an arbitrary origin, placed on the symmetry axis, the ellipsoids surface equations read:

$$\frac{\rho^2}{\frac{2V_0}{m_0\omega_{\rho_1}^2}} + \frac{(z + z_1)^2}{\frac{2V_0}{m_0\omega_{z_1}^2}} = 1, \quad \frac{\rho^2}{\frac{2V_0}{m_0\omega_{\rho_2}^2}} + \frac{(z - z_2)^2}{\frac{2V_0}{m_0\omega_{z_2}^2}} = 1, \tag{4}$$

where z_1 and z_2 are the absolute values of each of the two centers coordinates. Now the two oscillator potential expressions for deformed fragments come straightforward:

$$\begin{aligned} V_1(\rho, z) &= \frac{1}{2} m_0 \omega_{\rho_1}^2 \rho^2 + \frac{1}{2} m_0 \omega_{z_2}^2 (z + z_1)^2, \\ V_2(\rho, z) &= \frac{1}{2} m_0 \omega_{\rho_2}^2 \rho^2 + \frac{1}{2} m_0 \omega_{z_2}^2 (z - z_2)^2. \end{aligned} \tag{5}$$

What we have left to establish is the necking region potential, $V_g(\rho, z)$. The force that keeps nucleons confined within the ellipsoid is an attractive type one, radially inward ($\vec{F}_{ellipsoid} \sim -\vec{r}$). The same reason leads us to the hypothesis that, if nucleons are confined within the concave necking region,

which is geometrically *inversed* to the ellipsoid convex surface with respect to the centers of the fragments, a rejective force is needed, radially outward:

$$\vec{F}(\vec{r}) = -\beta\vec{r}, \tag{6}$$

hence a force oriented from outside the nuclear shape toward the surface. Then the corresponding potential is related to the expression:

$$\int_0^r \vec{F}d\vec{r} = \varphi(r) - \varphi(0) \tag{7}$$

or

$$\int_0^r \vec{F}d\vec{r} = \int_0^r -\beta\vec{r}d\vec{r} = -\frac{\beta r^2}{2}, \tag{8}$$

Consequently, $\varphi(r) = -\frac{\beta r^2}{2}$ is a potential form generating the rejective force. In this way, the rejective neck potential, defined up to a constant, must look like:

$$V_{g1}(r) = V_c + \varphi(r), \tag{9}$$

where V_c is a constant to be determined. On the nuclear surface S_g, we have again:

$$V_{g1} \mid_{S_g} = V_c + \varphi(r) \mid_{S_g} = V_0 \tag{10}$$

or

$$V_c = V_0 - \varphi(r) \mid_{S_g} . \tag{11}$$

For the sake of consistency, the rejective force is also considered of oscillator type:

$$\vec{F}(\vec{r}) = -m_0\omega_g^2\vec{r}, \tag{12}$$

therefore

$$\varphi(r) = -\frac{m_0\omega_g^2 r^2}{2}, \tag{13}$$

where the frequency ω_g has to be found. Since the potential must follow the geometrical shape, at the neck region the function $\varphi(r) = \varphi(\rho, z)$ reads:

$$\varphi(\rho, z) = -\frac{m_0\omega_g^2}{2}[(\rho - \rho_3)^2 + (z - z_3)^2] \tag{14}$$

and is centered in the middle of the neck sphere $O_3(\rho_3, z_3)$. On the neck surface then, where $(\rho, z) \in S_g$, we have:

$$\varphi(\rho, z) \mid_{S_g} = \frac{m_0\omega_g^2}{2}R_3^2 = V_{g1} \mid_{S_g} = V_0. \tag{15}$$

Then $V_c = V_0 - \varphi(r) \mid_{S_g} = 2V_0$ and the total neck potential from outside the shape down to the surface is:

$$V_{g1}(r) = 2V_0 - \frac{m_0\omega_g^2}{2}[(\rho - \rho_3)^2 + (z - z_3)^2] \tag{16}$$

and the neck frequency is directly related to the neck radius by Eq. (15). V_{g1} reach its maximum at the center of the neck sphere ($\rho = \rho_3$, $z = z_3$), where $V_{g1} = 2V_0$, then is decreasing down to the surface value $V_{g1} = V_0$ at a distance equal to the neck radius $(\rho - \rho_3)^2 + (z - z_3)^2 = R_3^2$ from O_3.

To complete the neck-dependent potential, there still remains the region inside the nuclear shape between the necking surface and the interior contours of the two spheroids. It can be observed that on the ellipsoids surface *inside* the shape the deformed oscillator potential has the same value as on the fragments surface, namely V_0. But on the surface of the shape within the necking region, the value is also V_0. Then, one concludes that inside the region volume between the neck surface and the two ellipsoids surfaces – $\rho_1(z) \leq \rho \leq \rho_g(z)$ and $\rho_2(z) \leq \rho \leq \rho_g(z)$ – the neck potential is constant.

$$V_{g2}(\rho, z) = cst = V_0. \tag{17}$$

Finally, the deformed oscillator potential part for the DTCSM reads:

$$V_{DTCSM}(\rho, z) = \\ = \begin{cases} V_1(\rho, z) = \frac{1}{2} m_0 \omega_{\rho_1}^2 \rho^2 + \frac{1}{2} m_0 \omega_{z1}^2 (z + z_1)^2, & v_1 \\ V_g(\rho, z) = \begin{cases} V_{g1}(\rho, z) = 2V_0 - [\frac{1}{2} m_0 \omega_g^2 (\rho - \rho_3)^2 + \frac{1}{2} m_0 \omega_g^2 (z - z_3)^2], & v_{g1} \\ V_{g2}(\rho, z) = V_0, & v_{g2} \end{cases} \\ V_2(\rho, z) = \frac{1}{2} m_0 \omega_{\rho_2}^2 \rho^2 + \frac{1}{2} m_0 \omega_{z_2}^2 (z - z_2)^2, & v_2 \end{cases} \tag{18}$$

where v_1, v_{g1}, v_{g2} and v_2 are the spatial regions where the corresponding potentials are acting.

Figure 2 shows how the three potentials work together. The values of $V_1(\rho, z)$, $V_2(\rho, z)$ and $V_{g1}(\rho, z)$ are taken at $\rho = \rho_1(z_{c1})$ (upper part of the figure), and $\rho = \rho_2(z_{c2})$, hence at the tangent points of the neck sphere. Evolution is shown as the distance R (or z-variable) increases. The values are taken at a matching surface point, thus the potentials are tangent all the time. One can observe how V_1 and V_2 wells are separating with increasing R. The matching surfaces are composed of the whole set of tangent points at every ρ distance from the symmetry axis.

4. EIGENFUNCTION BASIS

The new feature in the DTCSM eigenvalue problem is the shape-dependency of the potentials: V_{DTCSM}, the spin-orbit term $V_{\mathbf{\Omega s}}$ and the $V_{\mathbf{\Omega}^2}$ term ($\mathbf{\Omega}$ is preferred here as a notation since the angular momentum operator, as being

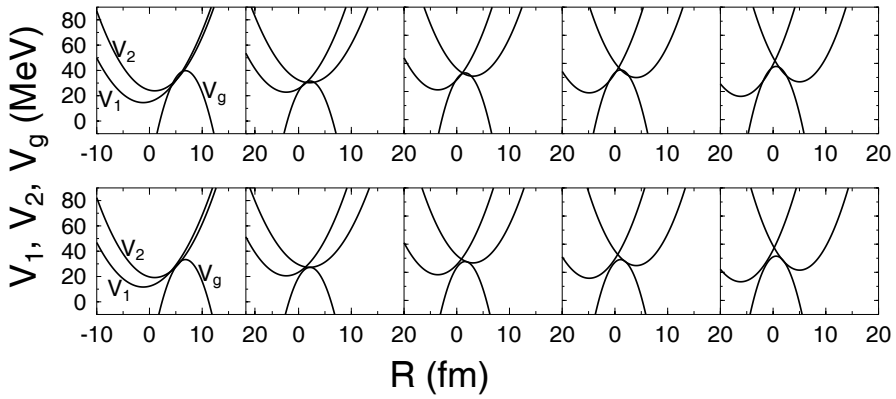

Fig. 2 – The evolution of the two fragments V_1 and V_2 and neck V_g potentials with the distance between centers at the tangent point of the neck with the heavy (upper plot) and light fragment.

shape dependent, will be different from the usual $\mathbf{l}$). The total Hamiltonian:

$$H_{DTCSM} = -\frac{\hbar^2}{2m_0}\Delta + V_{DTCSM}(\rho, z) + V_{\mathbf{\Omega s}} + V_{\mathbf{\Omega}^2} \tag{19}$$

is obviously not separable. A basis is needed and diagonalization of oscillator potential differences and of angular momentum dependent operators has to be performed.

A separable Hamiltonian is obtained if one takes $\omega_{\rho_1} = \omega_{\rho_2} = \omega_1$, with no $\mathbf{ls}$ and $\mathbf{l}^2$ terms, hence a potential like:

$$V^{(d)}(\rho, z) = \begin{cases} V_1^{(d)}(\rho, z) = \dfrac{1}{2}m_0\omega_1^2\rho^2 + \dfrac{1}{2}m_0\omega_1^2(z + z_1)^2, & z \leq 0 \\ V_2^{(d)}(\rho, z) = \dfrac{1}{2}m_0\omega_1^2\rho^2 + \dfrac{1}{2}m_0\omega_2^2(z - z_2)^2, & z \geq 0. \end{cases} \tag{20}$$

This is an appropiate two-center potential for a sphere ($z \leq 0$) intersected with a vertical spheroid. The origin ($z = 0$) is the intersection plane. As a result of variable separation, three known differential equations are obtained for harmonic functions, Laguerre polynomial and Hermite function dependent solutions [4].

Using continuity conditions for z-dependent functions and their derrivatives at $z = 0$, the normalization condition and equalizing the energy on the symmetry axis $E_z = \hbar\omega_1(\nu_1 + 0.5) = \hbar\omega_2(\nu_2 + 0.5)$, z-quantum numbers and normalization constants for the z-dependent eigenfunctions are calculated.

The ϕ and ρ-dependent functions are straitforward calculated from the differential equations. The final result is:

$$\begin{aligned}
\Phi_m(\phi) &= \frac{1}{\sqrt{2\pi}} \exp(im\phi) \\
R_{n_\rho}^{|m|}(\rho) &= \sqrt{\frac{2\Gamma(n_\rho+1)\alpha_1^2}{\Gamma(n_\rho+|m|+1)}} \exp\left(-\frac{\alpha_1^2\rho^2}{2}\right)(\alpha_1^2\rho^2)^{\frac{|m|}{2}} L_{n_\rho}^{|m|}(\alpha_1^2\rho^2) \qquad (21) \\
Z_\nu(z) &= \begin{cases} C_{\nu_1} \exp\left[-\frac{\alpha_1^2(z+z_1)^2}{2}\right] H_{\nu_1}[-\alpha_1(z+z_1)], & z<0 \\ C_{\nu_2} \exp\left[-\frac{\alpha_2^2(z-z_2)^2}{2}\right] H_{\nu_2}[\alpha_2(z-z_2)], & z\geq 0, \end{cases}
\end{aligned}$$

where Γ is the gamma function, L_n^m is the m-order Laguerre polynomial, C_1 and C_2 the normalization constants, ν_1, ν_2 the quantum numbers along the symmetry axis, and H_ν is the Hermite function. We now have a basis for further calculations. The eigenvalues for the diagonalized Hamiltonian with the potential $V^{(d)}$ are the oscillator energy levels for sphere+spheroid system:

$$E_{osc}^{(d)} = \hbar\omega_1(2n_\rho + \mid m \mid +1) + \hbar\omega_{z_1}(\nu_1 + 0.5). \qquad (22)$$

At this point we have a useful basis for the calculation of H_{DTCSM} matrix elements.

5. H_{DTCSM} OPERATORS

In order to obtain the DTCSM energy levels, the matrix of the non-diagonal elements should be constructed. Then, adding $E_{osc}^{(d)}$ as diagonal terms, after diagonalization we obtain the eigenvalues.

5.1. $V_{DTCSM}(\rho, z)$ – TERMS

This subsection is devoted to build the operators for the necked-in deformed two-center oscillator levels calculation. We start wiht the operators leading to the appropiate energies for $V_1(\rho, z)$. The difference $V_1(\rho, z) - -V^{(d)}(\rho, z)$ on the volume v_1 and added to $E^{(d)}(n_\rho, \nu, m)$ produce the suitable matrix elements for V_1:

$$\begin{aligned}
\Delta V_1 = \Delta V_1(-\infty, z_{im}) + \Delta V_1(z_{im}, 0) + \Delta V_1(0, z_{0m}+a_m) + \\
+\Delta V_1(z_{0m}+a_m, \infty) - \Delta V_1(z_{x1l} \div z_{c1}; \rho_{m1j} \div \rho_{m1s}) - \qquad (23) \\
-\Delta V_1(z_{c1} \div z_s; \rho_1 \div \rho_{m1s}) - \Delta V_1(z_s \div z_{mint}; \rho_m \div \rho_{m1s}).
\end{aligned}$$

The positive terms account for the influence of $V_1(\rho,z)$ as if V_1 would act alone everywhere but MPE. The negative terms are under $V_g(\rho,z)$ action. In parenthesis are the geometrical limits for every term. Note that for those which have also ρ-dependent limits, $\rho=\rho(z)$. What is left after the subtraction is the difference from $V_1(\rho,z)$ to $V^{(d)}(\rho,z)$ within the v_1 volume. To ease calculations, one uses as a notation:

$$\Delta V_1^{(p)}=\Delta V_1(-\infty,z_{im})+\Delta V_1(z_{im},0)+\Delta V_1(0,z_{0m}+a_m)+ \\ +\Delta V_1(z_{0m}+a_m,\infty). \tag{24}$$

These pozitive potential differences are now written in terms of the Heavyside step function; this will result in determining the exact limits where $V_1(\rho,z)$ is acting and, consequently, where it decides the oscillator energy values:

$$\Delta V_1^{(p)}=\frac{1}{2}(m_0\omega_{\rho_1}^2-m_0\omega_1^2)\{[1-\theta(z-z_{im})]+\theta[z-(z_{0m}+a_m)]\}\rho^2+ \\ +\frac{1}{2}\{(m_0\omega_{z_1}^2-m_0\omega_1^2)(z+z_1)^2[1-\theta(z-z_{im})]+ \\ +[m_0\omega_{z_1}^2(z+z_1)^2-m_0\omega_2^2(z-z_2)^2]\theta[z-(z_{0m}+a_m)]\}\delta_{n_{\rho'}n_\rho}+ \\ +\frac{1}{2}(m_0\omega_{\rho_1}^2-m_0\omega_1^2)\{[\theta(z-z_{im})-\theta(z)]+ \\ +[\theta(z)-\theta[z-(z_{0m}+a_m)]]\}\rho^2\theta(\rho-\rho_m(z))+ \\ +\frac{1}{2}\{(m_0\omega_{z_1}^2-m_0\omega_1^2)(z+z_1)^2[\theta(z-z_{im})-\theta(z)]+ \\ +[m_0\omega_{z_1}^2(z+z_1)^2-m_0\omega_2^2(z-z_2)^2][\theta(z)-\theta[z-(z_{0m}+a_m)]]\}\theta(\rho-\rho_m(z)). \tag{25}$$

To obtain the terms where the light emerged fragment potential $V_2(\rho,z)$ acts, one must subtract $V^{(d)}(\rho,z)$ from $V_2(\rho,z)$ within the v_2 volume. The result is:

$$\Delta V_2=\Delta V_2(z_{im}\div 0;0\div\rho_m(z))+\Delta V_2(0\div z_{0m}+a_m;0\div\rho_m(z))- \\ -\Delta V_2(z_s\div z_{c2};\rho_g(z)\div\rho_m(z))-\Delta V_2(z_{mint}\div z_{x2r};\rho_{m2j}(z)\div\rho_{m2s}(z)). \tag{26}$$

Let us denote:

$$\Delta V_2^{(p)}=\Delta V_2(z_{im}\div 0;0\div\rho_m(z))+\Delta V_2(0\div z_{0m}+a_m;0\div\rho_m(z)). \tag{27}$$

Then we have:

$$\Delta V_2^{(p)}=\frac{1}{2}(m_0\omega_{\rho_2}^2-m_0\omega_1^2)\{\theta[z-(z_{0m}+a_m)]\}\rho^2[1-\theta(\rho-\rho_m(z))]+ \\ +\frac{1}{2}\{[m_0\omega_{z_2}^2(z-z_2)^2-m_0\omega_1^2(z+z_1)^2][\theta(z-z_{im})-\theta(z)]+ \\ +(m_0\omega_{z_2}^2-m_0\omega_2^2)(z-z_2)^2\{\theta(z)-\theta[z-(z_{0m}+a_m)]\}\}[1-\theta(\rho-\rho_m(z))] \tag{28}$$

for the positive part; for the negative necking region which has to be subtracted from v_2, the expression for any $\Delta V_2(z_i \div z_f; \rho_i(z) \div \rho_f(z))$ is:

$$\Delta V_2(z_i \div z_f; \rho_i \div \rho_f(z)) =$$
$$= \frac{1}{2} m_0 \omega_{\rho 2}^2 [\theta(z - z_i) - \theta(z - z_f)] \rho^2 [\theta(\rho - \rho_i(z) - \theta(\rho - \rho_f(z))] +$$
$$+ \frac{1}{2} m_0 \omega_{z_2}^2 (z - z_2)^2 [\theta(z - z_i) - \theta(z - z_f)][\theta(\rho - \rho_i(z)) - \theta(\rho - \rho_f(z))] \quad (29)$$

using the same convention for z_i, z_f, ρ_i and $\rho_f(z)$ as for ΔV_1.

At this point, the neck potential $V_g(\rho, z)$ is filling its volume v_g without any subtraction:

$$\Delta V_g = V_g. \quad (30)$$

With the same notation as in Eq. (18) we have for the neck operators:

$$V_g = V_{g1}(v_{g1}) + V_{g2}(v_{g2}). \quad (31)$$

Now every of them will be taken separately:

$$V_{g1} = V_{g1}(z_{x1l} \div z_{c1}; \rho_{m1j} \div \rho_{m1s}) + V_{g1}(z_{c1} \div z_{mint}; \rho_g \div \rho_{m1s}) +$$
$$+ V_{g1}(z_{mint} \div z_{x2r}; \rho_{m2j} \div \rho_{m2s}), \quad (32)$$

$$V_{g2} = V_{g2}(z_{c1} \div z_s; \rho_1(z) \div \rho_g(z)) + V_{g2}(z_s \div z_{c2}; \rho_2(z) \div \rho_g(z)), \quad (33)$$

where again:

$$V_{g1}(z_i \div z_f; \rho_i \div \rho_f) = 2V_0[\theta(z - z_i) - \theta(z - z_f)][\theta(\rho - \rho_i(z)) - \theta(\rho - \rho_f(z))] -$$
$$- \frac{1}{2} m_0 \omega_g^2 [\theta(z - z_i) - \theta(z - z_f)](\rho - \rho_3)^2 [\theta(\rho - \rho_i(z)) - \theta(\rho - \rho_f(z))] -$$
$$- \frac{1}{2} m_0 \omega_g^2 (z - z_3)^2 [\theta(z - z_i) - \theta(z - z_f)][\theta(\rho - \rho_i(z)) - \theta(\rho - \rho_f(z))] \quad (34)$$

and

$$V_{g2}(z_i \div z_f; \rho_i \div \rho_f) = V_0\{[\theta(z - z_i) - \theta(z - z_f)][\theta(\rho - \rho_i(z)) - \theta(\rho - \rho_f(z))]\}. \quad (35)$$

6. SPIN-ORBIT ls AND l^2 OPERATORS

Because of the dependence of the angular momentum term on different space regions ($\sim \nabla V \times \mathbf{p}$), hence on different mass regions when asymmetry A_1/A_2 comes in, the anticommutator is used to assure hermicity for the operators:

$$V_{\mathbf{ls}} = \begin{cases} -\left\{ \dfrac{\hbar}{m_0 \omega_{01}} \kappa_1(\rho, z), (\nabla V \times \mathbf{p})\mathbf{s} \right\}, & A_1\text{-region} \\ -\left\{ \dfrac{\hbar}{m_0 \omega_{02}} \kappa_2(\rho, z), (\nabla V \times \mathbf{p})\mathbf{s} \right\}, & A_2\text{-region} \end{cases} \quad (36)$$

and

$$V_{\mathbf{l}^2} = \begin{cases} -\left\{\dfrac{\hbar}{m_0^2\omega_{01}^3}\kappa_1\mu_1(\rho,z),(\nabla V\times\mathbf{p})^2\right\}, & A_1\text{-region} \\ -\left\{\dfrac{\hbar}{m_0^2\omega_{02}^3}\kappa_2\mu_2(\rho,z),(\nabla V\times\mathbf{p})^2\right\}, & A_2\text{-region.} \end{cases} \tag{37}$$

Basically the same treatment as for oscillator terms is valid in this case. The $\kappa_1(\rho,z)$ and $\mu_1(\rho,z)$ are the strength function parameters for the $V_1(\rho,z)$ region, whereas $\kappa_2(\rho,z)$ and $\mu_2(\rho,z)$ are active for the $V_2(\rho,z)$ one.

The new feature here is the use of the anticommutator for the operators containing Heavyside function combinations, to confine the action to v_1, v_2 and v_g; these function combinations are exactly the ones which have been used for ΔV_1, ΔV_2 and ΔV_g terms.

Since the creation and anihilation angular momentum operators become shape-frequency dependent, notations will be changed as follows:

$$\mathbf{l}^+ \to \mathbf{\Omega}^+, \quad \mathbf{l}^- \to \mathbf{\Omega}^-, \quad \mathbf{l}_z \to \mathbf{\Omega}_z,$$

so that

$$\mathbf{ls} \to \frac{1}{2}(\mathbf{\Omega}^+\mathbf{s}^- + \mathbf{\Omega}^-\mathbf{s}^+) + \mathbf{\Omega}_z\mathbf{s}_z. \tag{38}$$

Then for the potentials of the spin-orbit term to be diagonalized one reads:

$$V_{\mathbf{\Omega s}} = V_{\mathbf{\Omega s}}(v_1) + V_{\mathbf{\Omega s}}(v_2) + V_{\mathbf{\Omega s}}(v_g), \tag{39}$$

$$V_{\mathbf{\Omega s}}(v_1) = -\frac{\hbar}{m_0\omega_{01}}\kappa_1\{\mathbf{\Omega s},(v_1)\}, \tag{40}$$

$$V_{\mathbf{\Omega s}}(v_2) = -\frac{\hbar}{m_0\omega_{02}}\kappa_2\{\mathbf{\Omega s},(v_2)\}, \tag{41}$$

$$V_{\mathbf{\Omega s}}(v_g) = -\frac{\hbar}{m_0\omega_{01}}\kappa_1\{\mathbf{\Omega s},(v_g^{(1)})\} - \frac{\hbar}{m_0\omega_{02}}\kappa_2\{\mathbf{\Omega s},(v_g)^{(2)}\}, \tag{42}$$

where $v_g^{(1)}$ and $v_g^{(2)}$ are the neck matching ellipsoids volumes on A_1 and A_2 side, respectively.

The necking spin-orbit operators terms in particular are:

$$\mathbf{\Omega}^+(v_{g1}) = -e^{i\varphi}\left[m_0\omega_g^2(\rho-\rho_3)\frac{\partial}{\partial z} - m_0\omega_g^2(z-z_3)\frac{\partial}{\partial\rho} - \frac{i}{\rho}m_0\omega_g^2(z-z_3)\frac{\partial}{\partial\varphi}\right]$$

$$\mathbf{\Omega}^-(v_{g1}) = e^{-i\varphi}\left[m_0\omega_g^2(\rho-\rho_3)\frac{\partial}{\partial z} - m_0\omega_g^2(z-z_3)\frac{\partial}{\partial\rho} + \frac{i}{\rho}m_0\omega_g^2(z-z_3)\frac{\partial}{\partial\varphi}\right]$$

$$\mathbf{\Omega}_z(v_{g1}) = im_0\omega_g^2\frac{\rho-\rho_3}{\rho}\frac{\partial}{\partial\varphi} \tag{43}$$

and $\mathbf{\Omega s}(v_{g2}) = 0$, since $V_g(v_{g2}) = V_0 = cst.$

Finally, the neck potential dependent spin-orbit interaction looks like:

$$V_{\mathbf{\Omega s}}(v_g) = -\frac{\hbar}{m_0\omega_{01}}\kappa_1\{\mathbf{\Omega s}(v_{g1}),(v_{g1}^{(1)})\} - \frac{\hbar}{m_0\omega_{02}}\kappa_2\{\mathbf{\Omega s}(v_{g1}),(v_{g1}^{(2)})\}, \quad (44)$$

where

$$\{\mathbf{\Omega s}(v_{g1}),(v_{g1}^{(1)})\} =$$
$$= \{\mathbf{\Omega s}(v_{g1}),[\theta(z-z_{x1l})-\theta(z-z_{c1})][\theta(\rho-\rho_{m1j}(z))-\theta(\rho-\rho_{m1s}(z))]\}+$$
$$+\{\mathbf{\Omega s}(v_{g1}),[\theta(z-z_{c1})-\theta(z-z_{mint})][\theta(\rho-\rho_g(z))-\theta(\rho-\rho_{m1s}(z))]\} \quad (45)$$

$$\mathbf{\Omega s}(v_{g1}),(v_{g1}^{(2)})\} =$$
$$= \{\mathbf{\Omega s}(v_{g1}),[\theta(z-z_{mint})-\theta(z-z_{x2r})][\theta(\rho-\rho_{m2j}(z))-\theta(\rho-\rho_{m2s}(z))]\}. \quad (46)$$

Now the total matrix elements for DTCSM can be calculated as:

$$\langle i|DTCSM|j\rangle = E_{osc}^{(d)}(n_\rho,|m|,\mu) + \langle i|\Delta V_1|j\rangle + \langle i|\Delta V_2|j\rangle + \langle i|V_g|j\rangle +$$
$$+\langle i|V_{\mathbf{\Omega s}}|j\rangle + \langle i|V_{\mathbf{\Omega}^2}|j\rangle. \quad (47)$$

7. LEVEL SCHEMES AND NECKING INFLUENCE ON SHELL EFFECTS

DTCSM spectra are computed for the superheavy fission reaction channel $^{306}122 \rightarrow ^{198}W + ^{108}Cd$, with the nuclei deformations $\chi_{122} = 0.9$, $\chi_W = 1.$ and $\chi_{Cd} = 0.83$. Semiaxes a_i and b_i are calculated from corresponding deformation parameter β_2 for every fragment, and using the volume conservation condition ($\beta_2^{^{198}W} = 0.$, $\beta_2^{^{108}Cd} = 0.135$). The reduced distance between centers is chosen to represent the elongation parameter of the shape: $(R - R_i)/(R_f - R_i)$, where R_i is the distance between centers when the light emerging fragment is completely embeded in the parent nucleus, and $R_f = a_1 + a_2 + 2R_3$ represents the final distance between centers, when the neck sphere is aligned with the fragments.

Five level schemes are drawn for five different neck parameters: $R_3 = 0; 1; 4; 7; 10$ fm in Fig. 3. The labels on the left of the first scheme correspond to the spherical level scheme, for $R_3 = 0$. The fact that levels do not converge for $p_{3/2}$, $d_{5/2}$, etc., is due to the slight deformation of the parent nucleus, which resulted from shell corrections calculations. Strong irregularities appear as R_3 increase, especially upon the states corresponding to higher energies. At intermediary stages of splitting ($(R - R_i)/(R_f - R_i) \approx 0.4 - 0.6$ there is an increase in higher level energies. This is due to the fact that the region where $V_g(\rho, z)$ is active becomes larger in volume; it is the moment to remember Fig. 2, which shows that potential inside the *neck-controlled* thorus is higher than the $V_1(\rho, z)$ and $V_2(\rho, z)$.

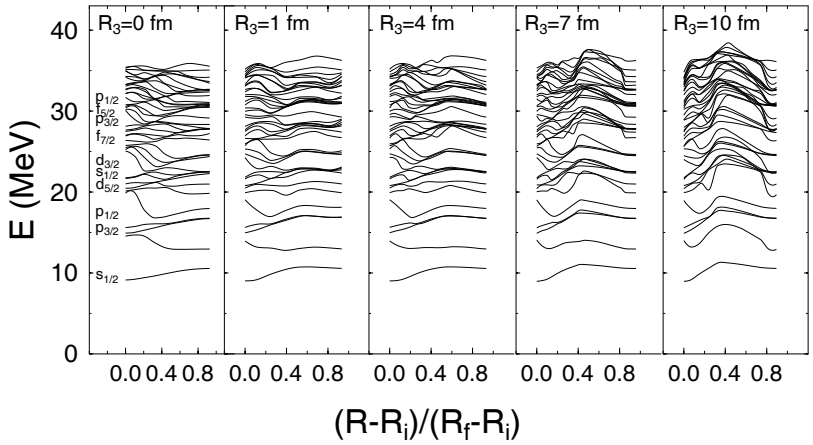

Fig. 3 – The level scheme corresponding to five values of the neck radius in $^{306}122 \rightarrow ^{198}W + ^{108}Cd$ reaction.

When one goes towards total splitting, the neck influence vanish little by little. As a result, the total potential is lower and the levels decrease their energies at $(R - R_i)/(R_f - R_i) \approx 0.9 - 1$. This behaviour is more obvious as R_3 is larger, when also contribution from $V_{g2} = V_0$, *inside* the shape span a larger region. It can be concluded that the neck-radius degree of freedom becomes more influential upon the single-particle energies in the last part of the overlapping region.

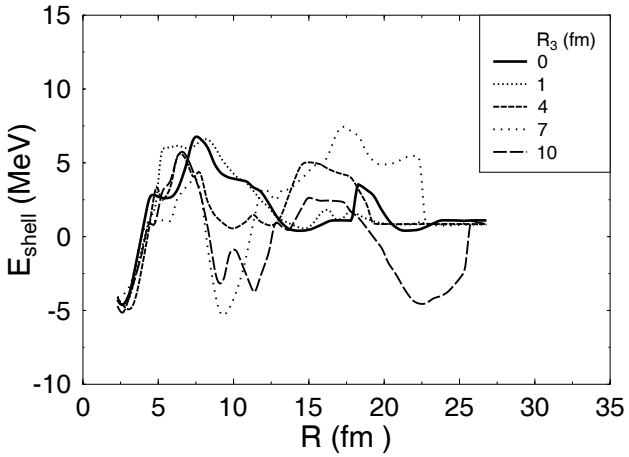

Fig. 4 – Shell corrections corresponding to the five level scheme in Fig. 3.

A direct consequence of the variation of the neck parameter R_3 on microscopic behaviour of a fission process is depicted in Fig. 4. Here the shell

corections are drawn for the five R_3 – parameter values, as a function of the distance between centers. They are calculated with the Strutinsky method. A shallow minimum at $R \approx 2.5$ fm suggest a small deformation of the $^{306}122$ ground state. First bump around $R \approx 5$ - 6 fm shows up in every case. Second bump is also there, but its position changes in R-value and in height (between $R = 12$ fm and $R = 20$ fm). The rather deep minimum (≈ -5 MeV) for large neck radii (apparent on the $R_3 = 10$ fm curve) is probably not manifested in $^{306}122$ fission, since at this distance between centers, the system is out of the fission barrier due to strong Coulombian repulsion.

8. **CONCLUSIONS**

The new necking-in dependent microscopic potential results in considering the neck degree of freedom into the level scheme calculation. As has been shown, the last part of the fision process is influenced by the difference in neck radii. This fact has important consequences on the potential barriers and fission paths on a potential energy surface calculated within more deformation degrees of freedom, necking included.

A new way of treating two partially overlapping nuclei has been introduced by making use of matching potential surfaces. It is only in this way that *continuity* between different regions of potential influence is assured. The potential pass smoothly from V_1 to V_g, to V_2 and so on without any cusp in its value and without the introduction of arbitrary geometric transition functions. For zero neck radius one obtains the fusion-like type of shapes.

All these facts make the presented model suitable for the study of fission channels and cluster decay phenomena and calculation of potential energy surfaces in fission.

REFERENCES

1. D.N. Poenaru, M. Ivascu and W. Greiner, *Fission and Beta-Delayed Decay Modes*, vol. III, CRC Press, Boca Raton, Florida, 1989.
2. D.N. Poenaru and W. Greiner, *Nuclear Decay Modes*, Ch. 6, Institute of Physics Publishing, Bristol, England, 1996.
3. D.N. Poenaru and M. Ivascu, Comp. Phys. Comm., **16**, 85 (1978).
4. E. Badralexe, M. Rizea and A. Sandulescu, Rev. Roum. Phys., **19**, 63 (1974).